Effect of Governor Deadbands on Valve Travel using Long-Term Dynamic Simulation

Thad Haines and Matt Donnelly
School of Mines and Engineering
Montana Technological University
Butte, Montana 59701

Abstract—Abstract goes here.

Index Terms—Governor deadbands, long-term dynamic simulation, time-sequenced power flow, valve travel

I. Introduction

Deadbands are commonly implemented in turbine speed governors to prevent a machine from responding to small frequency deviations that are ever present in electrical systems. Industry usage of deadbands is widely known, however, it is often overlooked in power system simulation. Incorporating governor deadbands into transient simulation models has been shown to generate results that better match measured power system events[1]. Additionally, numerous long-term operational benefits have been attributed to the alteration of deadband behavior[2]. To better understand how deadbands may affect system behavior, a long-term simulation would seem suitable. Long-term dynamic (LTD) simulation software focusing on governor dynamics was proposed in [3] and others, but has not been standardized nor fully developed.

This paper explores the impact of governor deadbands using a novel LTD simulation environment based on GE Energy's Positive Sequence Load Flow (PSLF) system models, dynamic data, and load flow solver. Valve travel as a metric for comparing the impact of various deadband scenarios is proposed. Section II describes the LTD simulation environment used to perform the studies. Section III discusses governor and deadband modeling within the simulation environment. In Section IV, the LTD simulation is validated against mature transient stability simulation. Finally, Section V presents some initial results demonstrating the viability of the proposed valve travel metric and Section VI offers conclusions.

II. Long-Term Dynamic Simulation Technique

Time-sequenced power flow (TSPF) is a method for LTD simulation proven to generate useful results[4]. The basic idea behind TSPF is to solve a power flow, perform system dynamics of interest, 're-seed' the power flow with new values, and repeat. A python based simulation software, Power System Long-Term Dynamic Simulator (PSLTDSim), has been developed to perform LTD simulations using TSPF. PSLTDSim has the ability to calculate system frequency, perform governor dynamics, model automatic generation control (AGC), and insert step, ramp, and noise type perturbances into a power system.

A. Simulation Assumptions and Simplifications

Due to the relatively large time steps of 1 second used with TSPF, numerous assumptions were made. Ideal exciters are assumed as modern exciters are typically fast enough to maintain reference voltage under stable conditions. Intermachine oscillations are ignored since the time resolution used is not fine enough to capture these phenomena.

Simplifications of transient stability models are used in PSLTDSim. The only parameters required to model a generator are MW cap, MVA base, and machine inertia. Additionally, a deadband modified tgov1 governor model, Fig. 1, was created to model system governors.
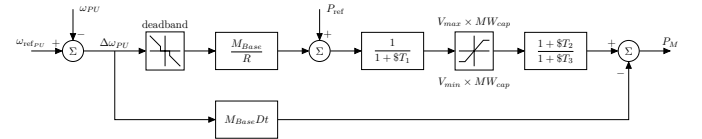

Fig. 1. Block diagram of modified tgov1 model.

B. Modeling the System-Wide Frequency Response

Instead of frequency being calculated for every bus, a combined swing equation is used to model only one system frequency. As shown in (1), accelerating power from the entire system, as well as total system inertia $H_{PU,sys}$, is used to calculate $\dot{\omega}_{sys}$.

$$\dot{\omega}_{sys} = \frac{1}{2H_{PU,sys}} \left(\frac{P_{accPU,sys}}{\omega_{sys}} - D_{sys}\Delta\omega_{sys} \right) \quad (1)$$

C. Distribution of Accelerating Power

In a system with N generators, total system accelerating power is calculated by

$$P_{acc,sys} = \sum_{i=1}^{N} P_{m,i} - \sum_{i=1}^{N} P_{e,i} \quad (2)$$

where $P_{m,i}$ is mechanical power and $P_{e,i}$ is electrical power of generator i.

System accelerating power is distributed to all generators in the system according to machine inertia as

$$P_{e,i} = P_{e,i} - P_{acc,sys}\left(\frac{H_i}{H_{sys}}\right) \quad (3)$$

where H has units of $MW \cdot s$.

The new value for $P_{e,i}$ is used in the next power flow solution for each generator. If the difference between expected and resulting power supplied by the slack generator is larger than a set slack tolerance, the difference is redistributed according to (3) until the resulting difference is below the slack tolerance, or a maximum number of iterations take place [5].

III. Implementation of Deadbands

FERC requirements for droop and deadband are 5% and 36 mHz respectively[6]. However, practical implementation is left to generator operators.

A. Types of Deadbands

Fig. 2 presents implementations of deadbands that follow FERC requirements. If a governor has no deadband, a change in output power is requested for any frequency deviation. A step deadband ignores any frequency smaller than the setpoint $\pm db_1$ and then steps to meet the set droop curve. A no-step deadband pushes the original droop curve away from the nominal frequency allowing for the droop curve to cross zero at $\pm db_2$ but never return to the step or no deadband droop curve. To avoid this alternate droop curve, a non-linear deadband is introduced that linearly increases from $\pm\alpha$ to $\pm\beta$, after which it follows the original droop curve.
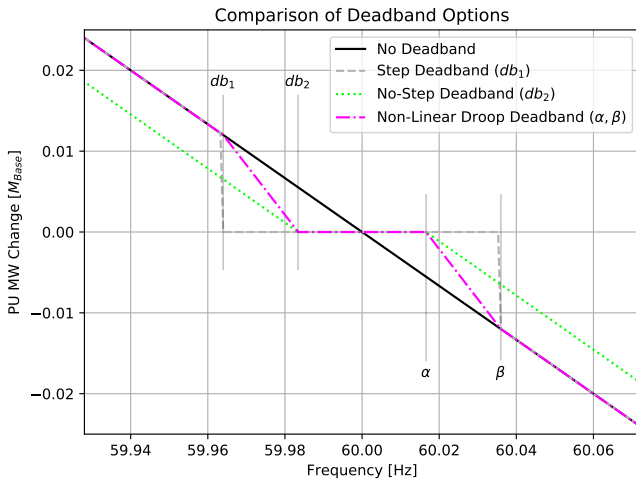

Fig. 2. Different types of deadbands.

IV. Simulation Validation

To validate the chosen simulation approach, identical system perturbances were performed in the PSLF Dynamic Subsystem (PSDS) and PSLTDSim. Frequency was compared to validate the single system frequency assumption calculated by PSLTDSim, and governed generator mechanical power was compared to validate governor action.

To simplify the comparison of frequency data from PSDS to LTD, a single weighted frequency based on generator inertia was calcualted using (4) and (5).

$$f_w = \sum_{i=1}^{N} f_i \frac{H_{PU,i} M_{base,i}}{H_{sys}} \quad (4)$$

$$\text{where } H_{sys} = \sum_{i=1}^{N} H_{PU,i} M_{base,i} \quad (5)$$

Due to the different time steps, when calculating the difference between PSDS and LTD, multiple PSDS values have the same held LTD value subtracted from them. For instance, any $\text{PSDS}(t = 3.x)$ value would have the $\text{LTD}(t = 3)$ value subtracted from it for comparison.

A. The MiniWECC System

The power system used for validation and valve travel experiments, the miniWECC shown in Fig. 3, is a 120 bus 34 generator system created in PSLF. All 21 governors in the miniWECC are modeled with the tgov1 which enabled easier validation. Further details about the creation and use of the miniWECC may be found in [7]–[9].
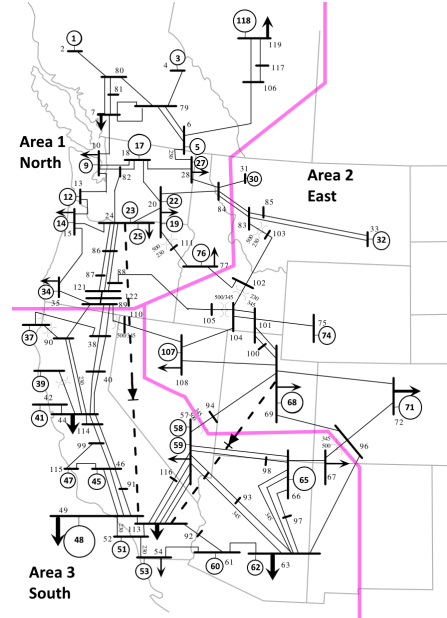

Fig. 3. MiniWECC system adapted from [9].

1) Load Step Results: A 400 MW load step was simulated to occur at 2 seconds. As shown in Fig. 4, all individual PSDS frequencies begin to oscillate after the perturbation while the weighted PSDS frequency appears to follow the general center of oscillation. The LTD system frequency is less oscillatory than the weighted frequency
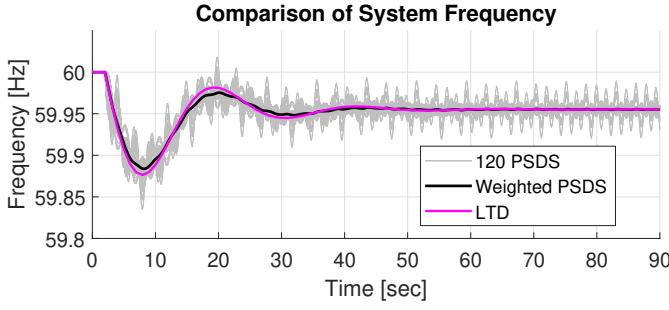
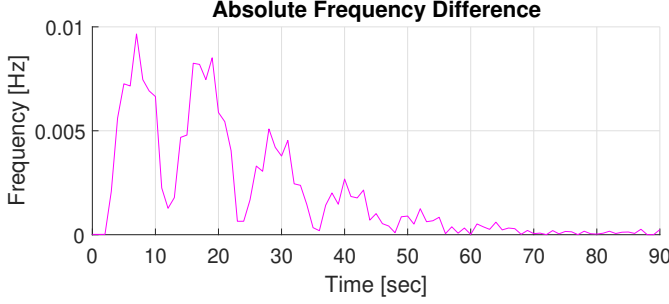Fig. 4. Comparison of frequency during load step.

Fig. 5. Absolute difference of weighted frequency during load step.

with only minor differences between the two. Fig. 9 quantifies these frequency differences.

When comparing mechanical power in Fig. 6, large MW differences can be seen, however, the percent difference data in Fig. 7 shows results less than 5% max difference, and an average percent difference of less than ≈0.5%.
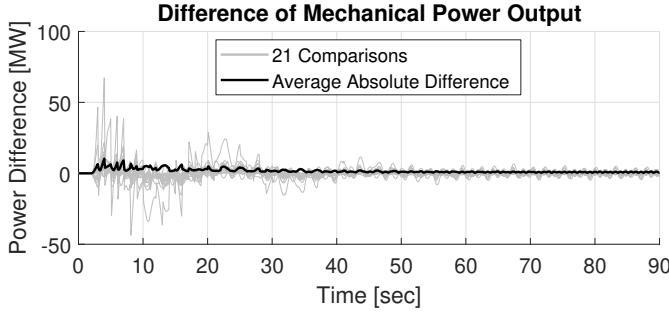

Fig. 6. Difference of mechanical power during load step.

2) Load Ramp Results: Simulation results from a 40 second 400 MW load ramp in Figs. 8-9 show frequency of LTD being within 1.2 mHz of PSDS. Fig.10 shows mechanical power differences of less than ±10 MW or, as Fig. 11 shows, 1% difference max.

B. Validation Summary

The step test results show that PSLTDSim is not meant to simulate large transient events with great accuracy. However, repeated small perturbances are modeled with acceptable deviation from transient simulation methods.
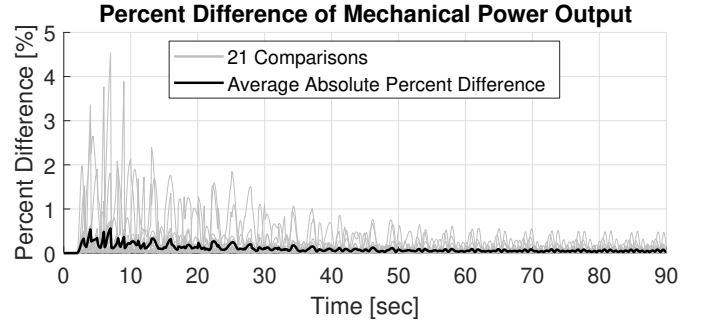

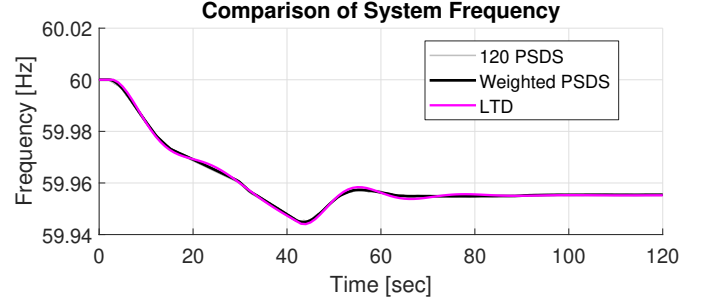Fig. 7. Percent difference of mechanical power during load step.

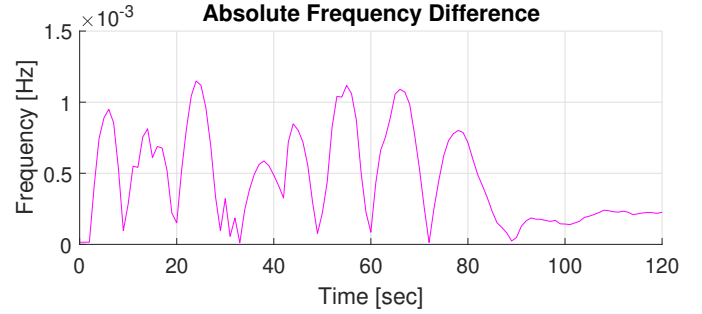Fig. 8. Comparison of frequency during load ramp.

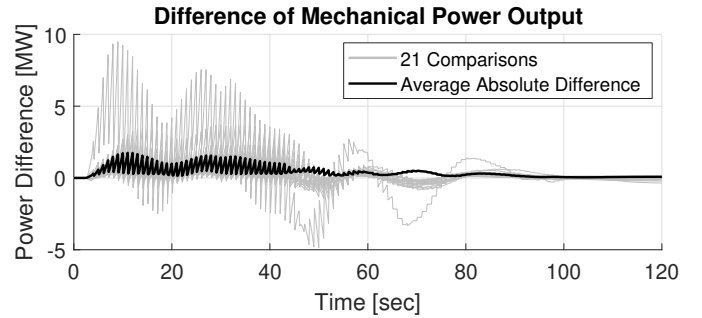Fig. 9. Absolute difference of weighted frequency during load ramp.

Fig. 10. Difference of mechanical power during load ramp.

V. Initial Results

Thirty minutes of random load noise was applied to the system where every governor in the system had an identical deadband. Each type of deadband shown in Fig.
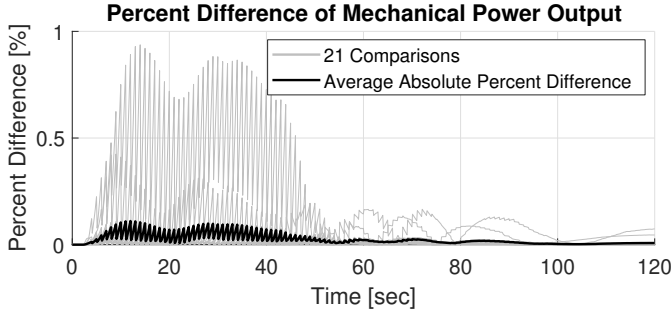
Fig. 11. Percent difference of mechanical power during load ramp.

Fig. 12. Total system loading.

Fig. 13. System frequency of various deadbands.

Fig. 14. Deadband valve movement comparisons.

2 was simulated. An experiment was also conducted to explore partial acceptance of the NERC recommendations presented in [2]. While PSLTDSim can model AGC, it was not enabled for these simulations.

A. System Modifications

The miniWECC system was modified to include three areas for simulation. PSLTDSim was used to set all area governor deadbands to 5%. Governors were removed from some units so that only ≈20% of generation capacity in each area had governor control.

B. System Noise Injection

Noise was injected into every load $P_{L,i}$ in the system according to

$$P_{L,i} = P_{L,i}(1 \pm N_Z Rand) \qquad (6)$$

where N_Z represents the maximum amount of random noise to inject as a percent, and *Rand* is randomly generated for each load as a number between 0 and 1 inclusive. The decision to add or subtract noise is chosen by another randomly generated number. As shown, (6) creates random walk behavior in load value that is representative of real power systems[3].

C. Noise Simulation Results

N_Z was set to 0.03 for all simulations. The noise added system loading is shown in Fig. 12 while Fig. 13 shows the resulting system frequency for each type of deadband. All linear deadband options maintain system frequency near their respective mHz setting until roughly minute 20. The step deadband option hold frequency almost exactly on the set deadband except when system loading decreases during minutes 7-11.

The first three minutes of a single generators valve travel are shown in Fig. 14 to compare how different deadbands affect movement. A step deadband will send pulse train-esq control signals to the governor valve when system frequency is oscillating over the deadband. These repeated control pulses greatly increase valve travel over the more linear deadband options. The no-step deadband matches valve movement of the no deadband case after an initial delay.
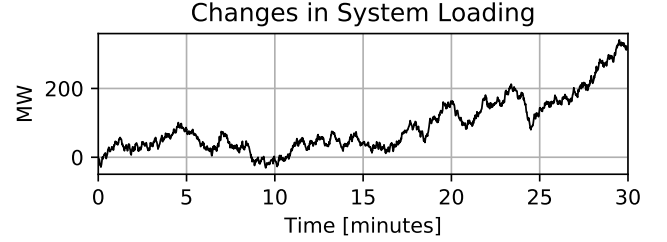
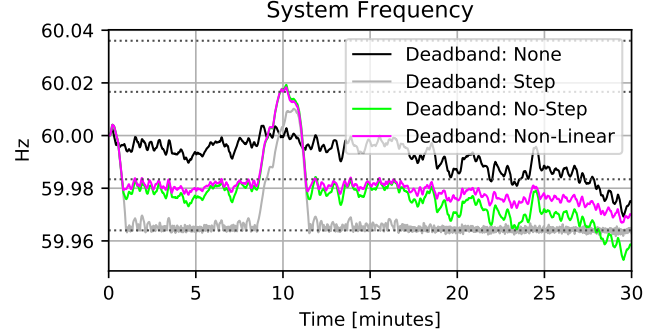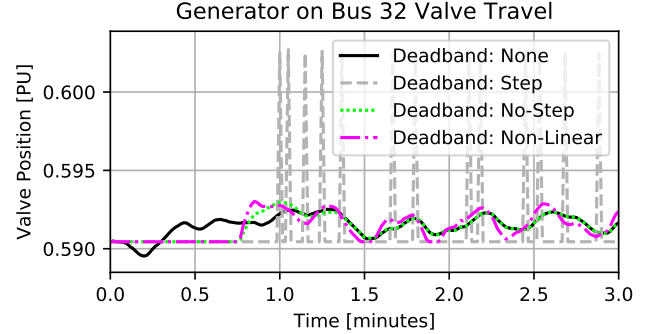Table I summarizes the valve travel for each generator in the system over the entire 30 minute simulation. A step type deadband has the largest total travel while the no deadband and no-step deadband cases are relatively similar. The non-linear droop deadband has slightly more movement than the no-step case, but also maintains a more nominal system frequency.

D. Universal Acceptance Simulation Results

To test partial acceptance of NERC recommendations, all area deadbands were set to the no-step variety, but two of the three areas had a deadband of 16.6 mHz while the third deadband was set to 36 mHz. The resulting system frequency is shown in Fig. 15.

TABLE I
Total valve travel for various deadband scenarios.

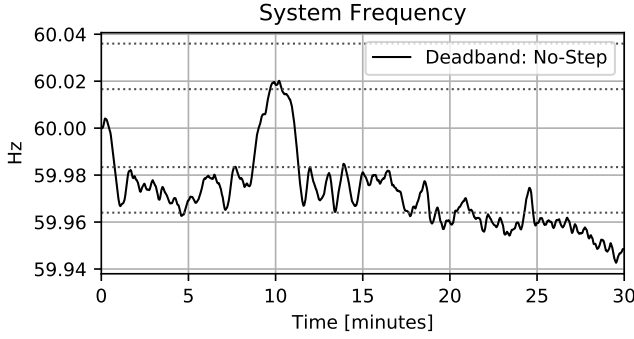|		Valve Travel [PU]		
Generator	No DB	Step	No-Step	N-L Droop
17	0.16	7.48	0.15	0.23
23	0.16	7.48	0.15	0.23
30	0.16	7.48	0.15	0.23
32	0.16	7.54	0.15	0.23
107	0.16	7.54	0.15	0.23
41	0.15	6.44	0.14	0.23
45	0.15	6.44	0.14	0.23
53	0.16	7.54	0.15	0.23
59	0.15	6.44	0.14	0.23
Total:	1.41	64.38	1.32	2.07

Fig. 15. System frequency to 0.03% load noise of no-step deadbands with different area settings.

As expected, Fig. 16 shows that the area with a larger deadband doesn't respond until after frequency drops below its deadband while the areas with smaller deadbands work to maintain frequency.
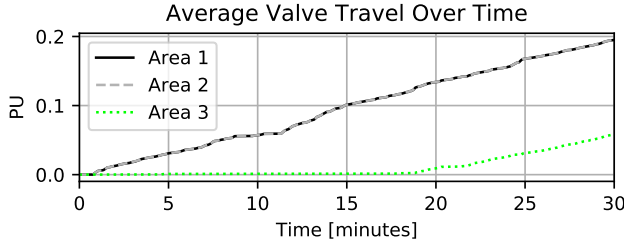

Fig. 16. Area average valve travel.

VI. Conclusion

Deadbands play a large role in dictating valve travel. A step deadband can lead to vastly increased valve travel compared to other, more linear, options. Smaller deadbands can reduce valve travel and help regulate frequency. However, in a system with a variety of deadbands, machines with smaller deadbands will respond more than machines with larger deadbands. This creates an uneven distribution of valve travel in a system. Therefore, if smaller deadbands are to be applied, they should be done interconnection wide to avoid unintentional inequalities in valve travel and associated machine wear.

References

[1] G. Kou, P. Markham, S. Hadley, T. King, and Y. Liu, "Impact of governor deadband on frequency response of u.s. eastern interconnection," IEEE Transactions on Smart Grid, 2016.

[2] NERC, "Frequency response initiative report," North American Electric Reliability Corporation, 2012.

[3] C. W. Taylor and R. L. Cresap, "Real-time power system simulation for automatic generation control," IEEE Transactions on Power Apparatus and Systems, 1976.

[4] E. Heredia, D. Kosterev, and M. Donnelly, "Wind hub reactive resource coordination and voltage control study by sequence power flow," IEEE, 2013.

[5] M. Stajcar, "Power system simulation using an adaptive modeling framework," Master's thesis, Montana Tech, 2016.

[6] FERC, "Essential reliability services and the evolving bulk-power system–primary frequency response," Federal Energy Regulatory Commission, Docket No. RM16-6-000 Order No. 842, Feb. 2018.

[7] D. Trudnowski, "Properties of the dominant inter-area modes in the wecc interconnect," Montana Tech, 2012.

[8] J. Sanchez-Gasca, M. Donnelly, R. Concepcion, A. Ellis, and R. Elliott, "Dynamic simulation over long time periods with 100% solar generation," Sandia National Laboratories, SAND2015-11084R, 2015.

[9] R. Hallett, "Improving a transient stability control scheme with wide-area synchrophasors and the microwecc, a reduced-order model of the western interconnect," Master's thesis, Montana Tech, 2018.